

Current-induced asymmetries of incompressible stripes in narrow quantum Hall systems

Rolf R. Gerhardt, Konstantinos Panos, and Jürgen Weis

Max-Planck-Institut für Festkörperforschung, Heisenbergstrasse 1, D-70569
Stuttgart, Germany

E-mail: R.Gerhardts@fkf.mpg.de

Abstract. We present recent experimental results confirming previously predicted strong asymmetries of the current distribution in narrow Hall bars under the conditions of the integer quantum Hall effect (IQHE). Using a previously developed self-consistent screening and transport theory of the IQHE, we investigate how these asymmetries, which are due to a non-linear feedback effect of the imposed current on the electron distribution in the sample, depend on relevant parameters, such as the strength of the imposed current, the magnetic field, the temperature, and the collision broadening of the Landau-quantized energy bands. We find that many aspects of the experimental results can be understood within this approach, whereas other aspects require explicit consideration of mechanism, which enforce the breakdown of the IQHE.

PACS numbers: 73.20.-r, 73.50.Jt, 71.70.Di

Submitted to: *New J. Phys.*

1. Introduction

Scanning force microscopy (SFM) [1] has provided interesting information [2, 3, 4] about the position dependence of Hall potential and current density in narrow Hall bars, with a width of about $10\ \mu\text{m}$. Under strong perpendicular magnetic fields B , which allow the observation of the integer quantized Hall effect (QHE) [5], three types of the spatial variation of the Hall potential were observed. For B values well outside the plateaus of the QHE, the Hall potential varied essentially linearly across the sample (“type I”), as one expects from the classical Drude theory of the Hall effect. As the B field entered a plateau region from the high-field side, a non-linear potential drop in a broad region in the middle of the sample was observed (“type II”). Most interestingly, near the low- B edges of the QH plateaus the Hall potential was constant in a broad region in the center of the sample and dropped across two strips that moved with decreasing B towards the sample edges (“type III”) [3]. Position and width of these strips coincided with those of the incompressible strips (ISs) expected to form in the sample due to the non-linear screening properties of the two-dimensional electron system (2DES) in strong magnetic fields [6, 7, 8, 9]. In the “perfect screening” limit [6, 7] of vanishing temperature and collision broadening, the potential varies only in these ISs, where the local filling factor is an integer and the electron density is constant, and in between the ISs the potential is flat.

These experimental results have been qualitatively reproduced by a self-consistent calculation [10] of the screened confinement potential $V(\mathbf{r})$ and the electron and current densities under the assumption, that the imposed, and in general dissipative, current density $\mathbf{j}(\mathbf{r})$ obeys a local form of Ohm’s law, $\mathbf{j}(\mathbf{r}) = \hat{\sigma}(\mathbf{r})\mathbf{E}(\mathbf{r})$, with the gradient of the electrochemical potential $\mu^*(\mathbf{r})$ as driving electric field, $\mathbf{E} = \nabla\mu^*/e$. The position-dependent conductivity tensor $\hat{\sigma}(\mathbf{r})$, determining longitudinal and Hall current, was, in turn, calculated from $V(\mathbf{r})$ and $\mu^*(\mathbf{r})$ under the assumption of *local thermodynamic equilibrium* [10]. Interestingly, these self-consistent calculations showed an unexpected non-linear feedback effect of the imposed current on the electron density: the calculated ISs near the sample edges, and as a consequence the current distribution among and the drop of the Hall potential across these strips, became with increasing strength of the imposed current increasingly asymmetric. However, since this asymmetry, which vanishes in the linear-response limit of low imposed current [11], was not clearly seen in the experiments, it was not investigated in detail.

In a recent series of similar experiments, SFM was applied to investigate the breakdown of the QHE in narrow Hall bars under strong imposed currents [12]. Unidirectional current pulses were used, to avoid averaging out of effects depending on the direction of the imposed current. Typical results, corresponding to the edge-determined “type III” behavior of Ref. [3], are shown in Fig. 1. Here the asymmetry of the steps in the Hall potential, caused by the current-carrying strips near the sample edges, is clearly seen, and the asymmetry increases with increasing strength of the imposed current. Experimental details and results for the “bulk-determined” situation

(corresponding to the “type I” and “type II” behavior of Ref. [3]) will be published separately [13]. In view of these new experiments it seems interesting to investigate in some detail the origin of these asymmetries, and their dependence on relevant parameters like temperature, strength of the imposed current, collision-broadening of the Landau levels, and, of course, the magnetic field value, which is important for existence and position of the ISs.

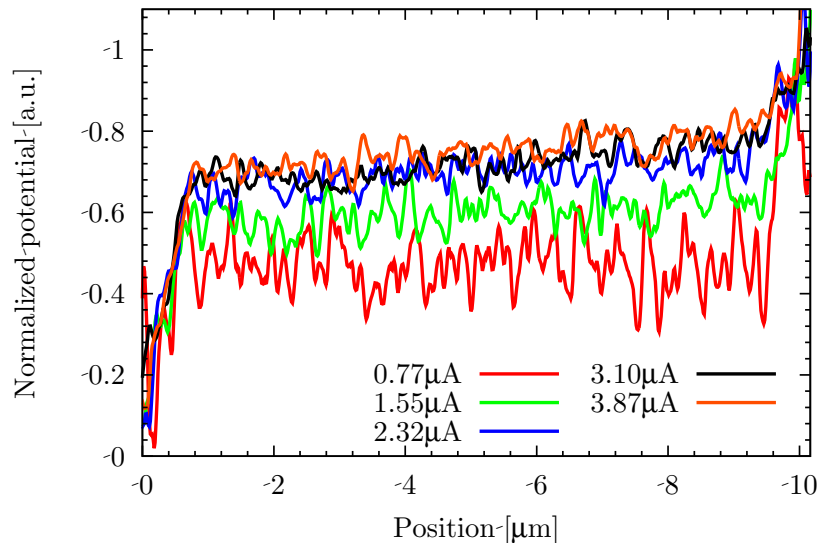


Figure 1. Normalized Hall potential measured on a $10\ \mu\text{m}$ wide Hall bar with electron density $n_{\text{el}} = 2.9 \cdot 10^{15}\text{m}^{-2}$ at $B = 5.6\text{T}$ (i.e., average Landau level filling factor $\nu = 2.14$). The asymmetry increases with increasing strength of the imposed current. From Ref. [12].

We should mention that current-induced asymmetries have also been predicted [14] for, and experimentally observed [15] in asymmetric Hall bars, with different profiles of confinement potential, and therefore electron density, at opposite edges. In such samples the shape of the quantized Hall plateaus changes, if the direction of the imposed current is reversed. These experiments indicate current-induced asymmetries, but provide no detailed information about the local distribution of the imposed current.

2. Model

In view of the unavoidable intrinsic fluctuations of the experimental data (see Fig. 1 and Ref. [3]), we will not attempt to reproduce them quantitatively, but only to achieve a qualitative understanding, and we will try to keep the model simple and the computer times short, following closely model assumptions and methods used in previous work [8, 9, 10, 11]. We have in mind a GaAs/(AlGa)As heterostructure containing a quasi 2DES, populated by a doping layer and laterally confined by top gates, but we assume the distances between the layers to be much smaller than the width of the 2DES, and neglect them. Thus we assume that all charges, including induced gate-charges, reside in the plane $z = 0$ [6, 7, 8, 9], and we model the Hall bar as a 2DES in that plane, being translation invariant in y direction and confined in x direction to the stripe $|x| < d$. We neglect exchange and correlation effects and spin-splitting, and we replace the mutual Coulomb interaction between the electrons

by an effective Hartree potential, determined by the density $n_{\text{el}}(x)$ of the 2DES. With the boundary conditions $V(x, z) \rightarrow 0$ for $|z| \rightarrow \infty$ and $V(x, 0) = V_L$ for $x < -d$ and $V(x, 0) = V_R$ for $x > d$ the potential $V(x, z)$ is obtained as an integral over the charge density in the stripe $|x| < d$ [10]. A constant density n_D of ionized donors (Si^+) in $|x| < d$ contributes $V_D(x) = -E_D[1 - (x/d)^2]^{1/2}$, with $E_D = 2\pi e^2 n_D d / \bar{\kappa}$, to the effective confinement potential $V(x, 0) = V(x) = V_D + V_g + V_H$, a gate voltage $V_R - V_L$ contributes $V_g(x) = (V_L + V_R)/2 + (V_R - V_L) \arcsin(x/d)/\pi$, and $V_H(x) = (2e^2/\bar{\kappa}) \int_{-d}^d dx' K(x, x') n_{\text{el}}(x')$ is the Hartree potential, determined by the kernel

$$K(x, x') = \ln \left| \frac{\sqrt{(d^2 - x^2)(d^2 - x'^2)} + d^2 - x'x}{(x - x')d} \right|. \quad (1)$$

Here $V(x)$ is normalized to give the potential energy of an electron, and $\bar{\kappa}$ is an effective dielectric constant [10, 11].

To obtain self-consistency, we have to calculate $n_{\text{el}}(x)$ from $V(x)$. The full Hartree approximation requires to solve the eigenvalue problem with the potential $V(x)$, but we assume that $V(x)$ varies within the 2DES slowly on the scale of the magnetic length $\ell_B = \sqrt{\hbar c / eB}$. This allows to approximate the energy eigenvalue of the Landau state with center coordinate X by $E_n(X) = V(X) + E_n$, with E_n the Landau energy without confinement, and to neglect the extent of the states in x -direction, when calculating the density [16]. This leads in thermal equilibrium to the Thomas-Fermi approximation

$$n_{\text{el}}(x) = \int dE D(E) f([E + V(x) - \mu^*] / k_B T), \quad (2)$$

with $f(\varepsilon) = 1/[1 + \exp(\varepsilon)]$ the Fermi function, k_B Boltzmann's constant, T the temperature, and $D(E)$ the density of states (DOS) in the absence of the confinement potential. We take $D(E) = D_0 = m/(\pi\hbar^2)$ for $B = 0$, and for large, quantizing magnetic fields $D(E) = \sum_{n=0}^{\infty} A_n(E)/(\pi\ell_B^2)$ with the Gaussian form $A_n(E) = \exp(-[E_n - E]^2/\Gamma^2)/(\sqrt{\pi}\Gamma)$ of the spectral function [17], with $\Gamma = \gamma\hbar\omega_c[10\text{T}/B]^{1/2}$ and γ a measure of the collision broadening. Here $E_n = \hbar\omega_c(n + 1/2)$ are the Landau energies with $\omega_c = eB/mc$ the cyclotron frequency, m is the effective mass, and we assume spin-degeneracy. Figure 2 shows typical thermal-equilibrium results for a sample with gate distance $2d = 3\mu\text{m}$ and with $N \sim 500$ equidistant mesh points for the evaluation of integrals. (Results for $d = 2.5\mu\text{m}$ and $N \sim 1000$ are very similar). In view of the experiments [12], we have chosen a donor density of $n_D = 4 \cdot 10^{11}\text{cm}^{-2}$, so that with the GaAs values $m = 0.067m_0$ and $\bar{\kappa} = 12.4$ the minimum of $V_D(x)$ is $V_D(0) = -E_D = -4.38\text{eV}$. For $B = 0$ and $T = 0$ we confine the electron density to the stripe $|x| < 0.9d$, solve the resulting linear integral equation [10], and obtain a symmetric density profile with an average electron density $\bar{n}_{\text{el}} = 2.90 \cdot 10^{11}\text{cm}^{-2}$. The resulting confinement potential vanishes on the gates, $V_L = V_R = V(\pm d) = 0$ and is well screened within the 2DES, with minimum $V(0) = -0.71\text{eV}$, and the electrochemical potential is $\mu^* = -0.70\text{eV}$, so that the total potential varies within the 2DES only by about 10 meV (see black lines of Fig. 2). Starting with these values, the Newton-Raphson method with stepwise temperature changes [10] was used to obtain results for

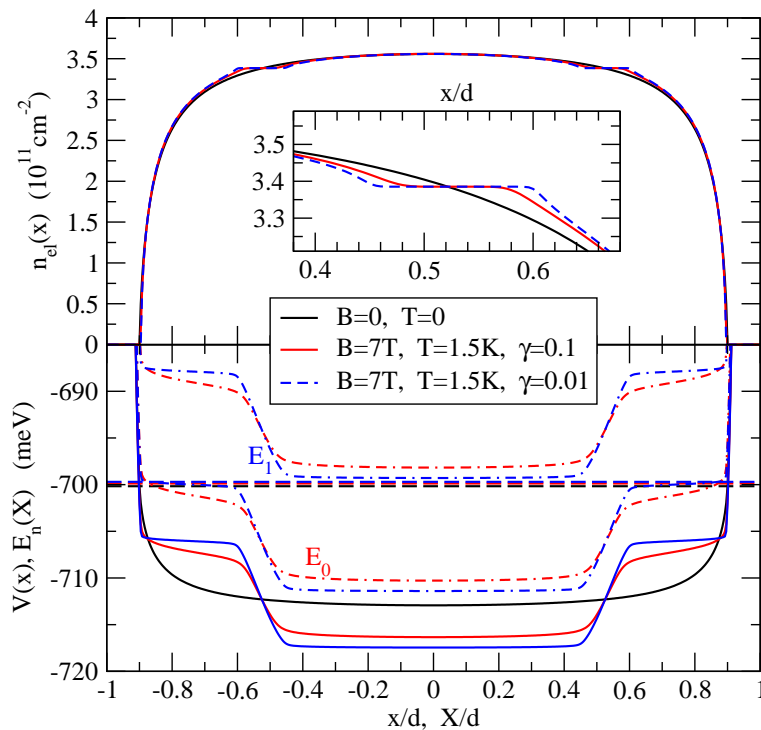


Figure 2. Self-consistent potential and electron density in thermal equilibrium. Black lines: $B = 0$, $T = 0$; other lines for $B = 7\text{ T}$, $T = 1.5\text{ K}$, and Gaussian spectral functions of width $\Gamma = \gamma \hbar \omega_c [10\text{ T}/B]^{1/2}$, with $\gamma = 0.1$ (red), and $\gamma = 0.01$ (blue), respectively; broken lines: μ^* , dash-dotted: Landau energies.

high magnetic fields and low temperatures. The pinning of the Landau levels to the constant electrochemical potential becomes more effective for smaller γ and, of course, for lower T . The current $-e\langle n, X | \hat{v}_y | n, X \rangle = (e/m\omega_c)dE_n(X)/dX$ carried by the state $|n, X\rangle$ reduces in our approximation to $(c/B)dV(X)/dX$, so that the intrinsic (Hall) currents in the perfect screening limit are confined to the incompressible strips, with opposite current directions near opposite sample edges, and vanish in the compressible regions of constant potential.

To describe a *stationary non-equilibrium state* with an imposed current I along the Hall bar, we assume *local equilibrium* and replace the constant electrochemical potential μ^* in Eq. (2) by a position-dependent one, $\mu^*(x, y)$. As in Ref. [10] we assume, that the current density obeys Ohm's law with the driving electric field $\mathbf{E} \equiv \nabla\mu^*/e$ and position-dependent conductivity tensor components $\sigma_{xx}(x) = \sigma_{yy}(x) = \sigma_\ell(x)$ and $\sigma_{yx}(x) = -\sigma_{xy}(x) = \sigma_H(x)$. To maintain translation invariance in y -direction, $\mathbf{E}(x, y)$ must be independent of y . In a stationary state we have $\nabla \cdot \mathbf{j} = 0$ and $\nabla \times \mathbf{E} = \mathbf{0}$, so that the current density j_x across and the field E_y along the Hall bar are independent of x , $j_x(x) \equiv j_x^0$ and $E_y(x) \equiv E_y^0$. Then the electrochemical potential assumes the form $\mu^*(x, y) = \mu^*(x) + eE_y^0 y$ and, in order to guarantee the translation invariance of the electron density, we must add the term $eE_y^0 y$ also to the confinement potential (where it describes the effect of a source-drain voltage along the Hall bar), so that the difference $V(x, y) - \mu^*(x, y) = V(x) - \mu^*(x)$ is independent of y .

In the following we assume sufficiently wide depletion strips between the 2DES and the gates, so that the current across the Hall bar vanishes, $j_x^0 = 0$. Then the remaining current and field components are easily expressed in terms of the resistivity components

$\rho_\ell(x) = \sigma_\ell(x)/[\sigma_\ell(x)^2 + \sigma_H(x)^2]$ and $\rho_H(x) = \sigma_H(x)/[\sigma_\ell(x)^2 + \sigma_H(x)^2]$ as

$$j_y(x) = E_y^0/\rho_\ell(x), \quad E_x(x) = \rho_H(x) j_y(x), \quad (3)$$

resulting in $\mu^*(x, y) = eE_y^0 y + \mu^*(x)$ with

$$\mu^*(x) = \mu_0^* + eE_y^0 \int_0^x dx' \rho_H(x')/\rho_\ell(x'). \quad (4)$$

Here μ_0^* occurs as constant determining the average electron density, and E_y^0 is determined by the relation $\int_{-d}^d dx j_y(x) = I$ as $E_y^0 = I/\int_{-d}^d dx [1/\rho_\ell(x)]$. If in the limit $T \rightarrow 0$ an IS develops where $\rho_\ell(x) \rightarrow 0$, the last integral diverges, i.e., the electric field and the resistance along the Hall bar vanish, and the sample will show the QHE.

For the sake of comparison, we recall the classical Drude model

$$\rho_\ell^D(x) = m/[e^2 \tau n_{\text{el}}(x)], \quad \rho_H^D(x) = \omega_c \tau \rho_\ell(x), \quad (5)$$

with a constant scattering time τ , which according to Eq. (3) leads to a current density proportional to the electron density, $j_y^D(x) \propto n_{\text{el}}(x)$, and to a constant Hall field $E_x^D = \omega_c \tau E_y^0$.

In the following we include Landau quantization and Shubnikov-de Haas effect by taking as model for the conductivity tensor [10]

$$\begin{aligned} \sigma_H(x) &= (e^2/h)\nu(x), & \nu(x) &= 2\pi\ell_B^2 n_{\text{el}}(x), \\ \sigma_\ell(x) &= \frac{e^2}{h} \int_{-\infty}^{\infty} dE [-f'_E] \sum_{n=0}^{\infty} (2n+1) [\sqrt{\pi}\Gamma A_n(E)]^2, \end{aligned} \quad (6)$$

where $n_{\text{el}}(x)$ is calculated according to Eq. (2) with the argument of the Fermi function replaced by $[E + V(x) - \mu^*(x)]/k_B T$ and where $f'_E = \partial f([E + V(x) - \mu^*(x)]/k_B T)/\partial E$. To obtain reasonable results for the Hall voltage, we follow Ref. [10] and require that the induced charges on each gate remain constant, independent of the imposed current I . For the gate at $x > d$ this requires to fix [10]

$$Q_R = \frac{2e}{\pi} \int_{-d}^d dx [n_D - n_{\text{el}}(x)] \arctan \sqrt{\frac{d+x}{d-x}}. \quad (7)$$

We modify the previous approach [10] in two respects. First, we avoid the cutoff $\sigma_\ell(x) > \epsilon \cdot \sigma_H(x)$ with $\epsilon = 10^{-4}$ used in Ref. [10], since it becomes crucial already for relevant values of temperature and collision broadening, and makes the results for the current density in the incompressible strips unreliable. The second modification has been introduced [11] and discussed [16, 14] previously. The Thomas-Fermi approximation (TFA), which neglects the spatial extent of the Landau eigenstates, and the assumption of a strictly local form of Ohm's law, which is reasonable on a length scale much larger than the average electron separation, lead to physical and mathematical problems. A simple and reasonable way to overcome these problems is to replace in Ohm's law the conductivity tensor $\hat{\sigma}(x)$, calculated within the local thermal equilibrium approach, by a smoothed form [11, 16]

$$\hat{\sigma}(x) = \frac{1}{2\lambda} \int_{-\lambda}^{\lambda} d\xi \hat{\sigma}(x + \xi). \quad (8)$$

We will investigate the effect of this averaging in addition to that of temperature, collision broadening, current strength, and magnetic field.

3. Results

Low-temperature results with imposed current were obtained following two routes. In the first, we start with the equilibrium state ($I = 0$) at low temperature and increase the current stepwise. For given I , we first keep $\mu^*(x) - \mu_0^*$ fixed and calculate $V(x)$ and $n_{\text{el}}(x)$ as in equilibrium, determining μ_0^* and $V_R - V_L$ so that the average electron density \bar{n}_{el} and the induced gate charge Q_R , Eq. (7), remain unchanged. Then we calculate for the resulting $V(x) - \mu^*(x)$ the conductivities, Eqs. (6), and via Ohm's law and Eq. (4) a new $\mu^*(x) - \mu_0^*$. This procedure is iterated until the changes of $V(x)$ and $\mu^*(x)$ are negligible. The next value of I is treated in the same way.

Figure 3 shows corresponding results for $I = 0$ and $I = 0.5 \mu\text{A}$ at $T = 4 \text{ K}$. Similar results have been presented in Ref. [14], but without details of the current density $j_y(x)$, which decreases by several orders of magnitude already inside the ISs. Note the

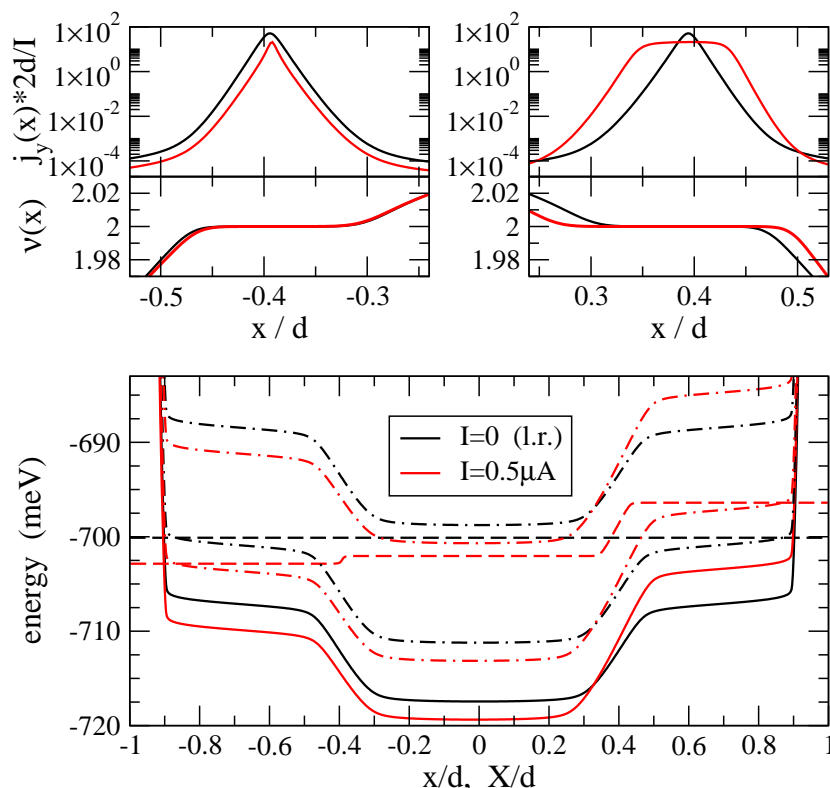


Figure 3. Lower part: self-consistent potential $V(x)$ (solid lines), electrochemical potential $\mu^*(x)$ (broken lines), and Landau energies $E_n(X)$ (dash-dotted); upper parts: density $j_y(x)$ of imposed current and filling factor $\nu(x)$ near the incompressible strips; $B = 7.2 \text{ T}$, $T = 4 \text{ K}$, $\gamma = 0.01$, $N = 980$.

logarithmic scale for $j_y(x)$, which shows the symmetric linear response result for $I = 0$ and the strongly asymmetric result for $I = 0.5 \mu\text{A}$. Outside the ISs $j_y(x)$ is at least about five orders of magnitude smaller than in their centers. As a consequence, the ‘‘Hall potential’’ $\mu^*(x)$ is practically constant outside the ISs. In the IS near $x = 0.4d$ the imposed current has the same direction as the intrinsic current. This leads to an increase of the potential variation across and a broadening of this strip, whereas the

IS near $x = -0.4d$ is much less affected. As a consequence, the variation of the Hall potential across the IS near $x = 0.4d$ is larger than that across the IS near $x = -0.4d$. Since we prohibit charge transfer between the gates, i.e. keep Q_R constant, a gate voltage $(V_R - V_L)/e = [V(d) - V(-d)]/e = 10.795$ mV builds up, which is considerably larger than the calculated Hall voltage $U_H = [\mu^*(d) - \mu^*(-d)]/e = 6.4532$ mV, satisfying $U_H = R_H(2)I$ with the quantized Hall resistance $R_H(2) = 0.5 h/e^2 \hat{=} 12.9064$ k Ω at filling factor $\nu = 2$. These results depend, of course, on the direction of the imposed current I . Since the considered sample is symmetric without imposed current, $n_{\text{el}}(-x) = n_{\text{el}}(x)$, $V(-x) = V(x)$, etc., we obtain for the symmetry due to the non-linear feedback of I

$$n_{\text{el}}(x; -I) = n_{\text{el}}(-x; I), \quad j_y(x; -I) = -j_y(-x; I). \quad (9)$$

The normalized Hall potential $H(x) = \Delta(x)/\Delta(d)$ with $\Delta(x) = \mu^*(x) - \mu^*(-d)$, plotted in Figs. 4 - 6, changes under inversion of I as $H(x; -I) = 1 - H(-x; I)$.

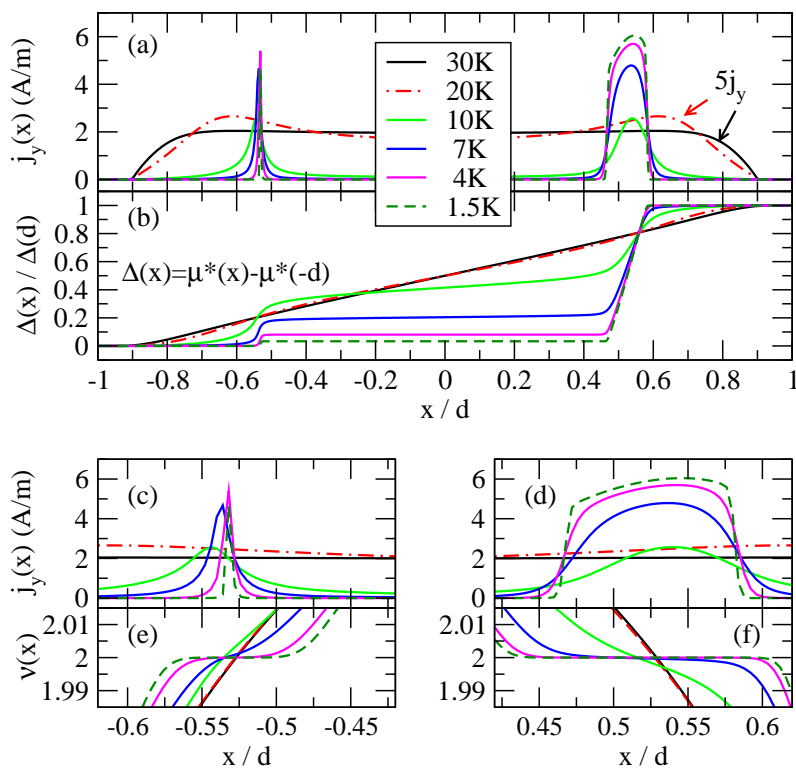


Figure 4. Position dependence of current density $j_y(x)$, (a), and normalized Hall potential, (b), for different temperatures, from $T = 30$ K to $T = 1.5$ K. Details of $j_y(x)$ and of $\nu(x)$ near the positions of incompressible strips are shown in (c) and (d), and in (e) and (f), respectively; $B = 7$ T, $\Gamma/\hbar\omega_c = 0.12$, imposed current $I = 1$ μ A.

Another route to the same results is to introduce the current at high temperature and then to lower T stepwise, keeping B and I constant. A typical result is shown in Fig. 4 for a relatively high imposed current, $I = 1$ μ A. At sufficiently high temperature, $T \gtrsim 30$ K, the current density $j_y(x)$ is proportional to the electron density $n_{\text{el}}(x)$, which drops monotonously from the center towards the edges, and the Hall voltage, Fig. 4(b), varies linearly across the sample. At low temperature, $T \lesssim 4$ K, $n_{\text{el}}(x)$ develops very asymmetric plateaus with local filling factor $\nu(x) = 2$, see Fig.4 (e) and (f), and $j_y(x)$ is confined to these plateaus, where $\sigma_{\ell}(x)$ and therefore the dissipation becomes small. As a consequence, the Hall potential drops asymmetrically across these plateaus and becomes constant outside.

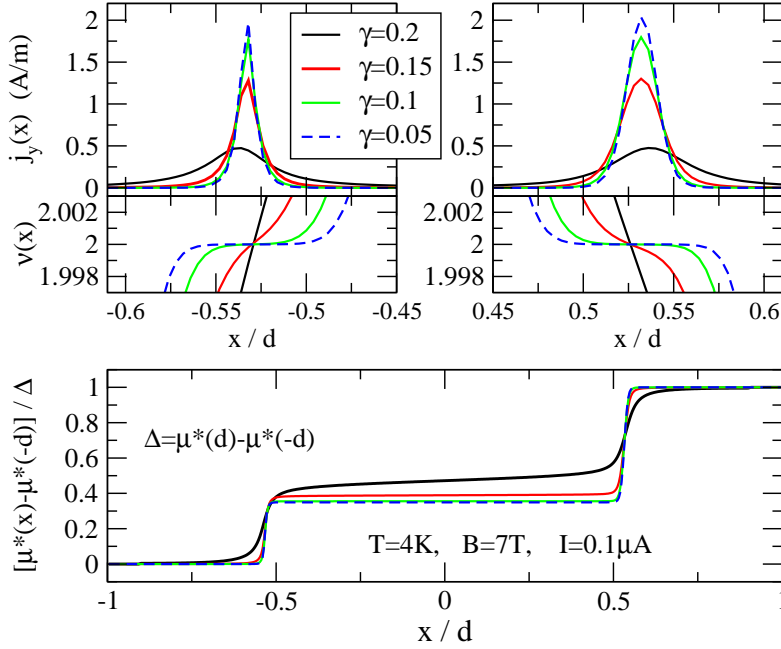


Figure 5. Normalized Hall potential, current density $j_y(x)$, and $\nu(x)$ as in Fig. 4, but for $T = 4\text{K}$, $I = 0.1\mu\text{A}$, and different values of collision broadening.

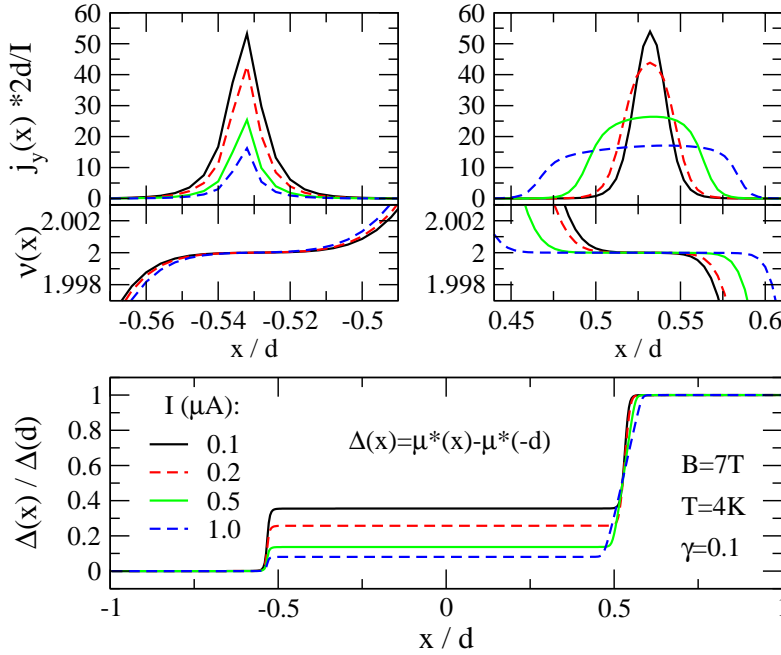


Figure 6. Normalized Hall potential, $j_y(x)$, and $\nu(x)$ as in Fig. 4, but for $T = 4\text{K}$, $\gamma = 0.1$, and different values of the imposed current I .

Figure 5 shows, for a weaker current, that the asymmetry decreases with increasing collision broadening. Apparently the current is already largely concentrated in the regions with local filling factor $\nu(x) \approx 2$ before pronounced plateaus and ISs develop. As shown in Fig. 6, the width of the IS and the $j_y(x)$ peak near $x/d = 0.53$ increase considerably with increasing imposed current I , whereas the corresponding width near $x/d = -0.53$ shrinks only a little (note the different scales of the left and the right parts of Fig. 6).

So far we have considered situations in which, for sufficiently low T and small γ , we found well developed ISs. Figure 7 shows that the corresponding B -fields ($\sim 7\text{T}$)

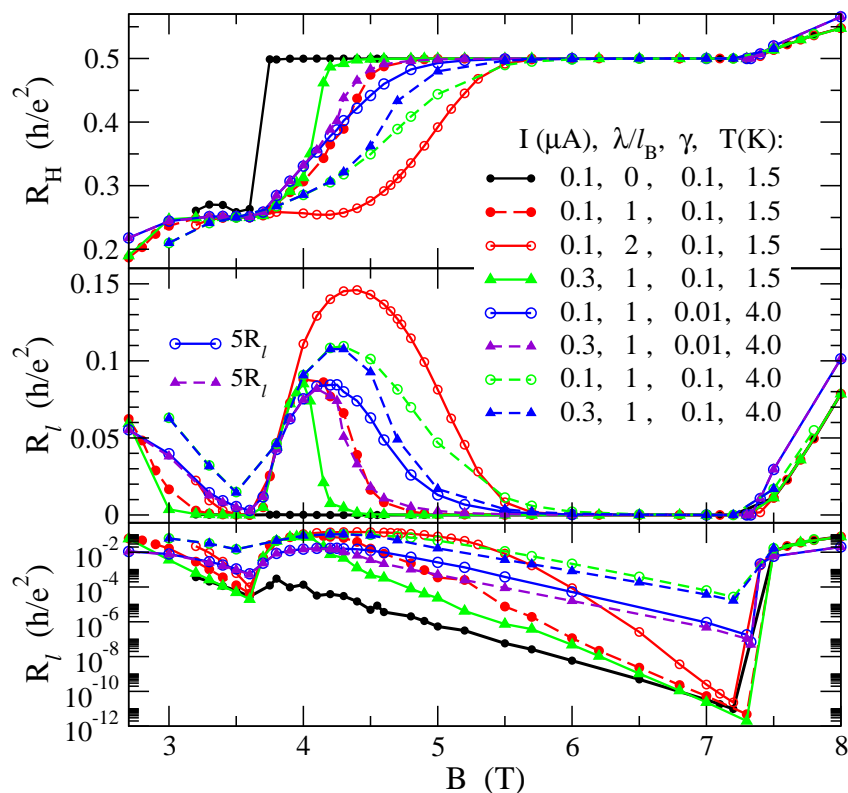


Figure 7. B -dependence of Hall resistance $R_H = [\mu^*(d) - \mu^*(-d)]/(eI)$ (upper part) and longitudinal resistance $R_\ell = E_y^0 2d/I$ in linear (middle) and logarithmic scale (lower part), for different values of imposed current I , smoothing length λ (in units of the magnetic length), collision broadening γ , and temperature T .

are located in the $\nu = 2$ QH plateau near its high- B edge. Before we consider other situations, we recall a problem of the approach discussed so far [11]. As B is lowered, the ISs move towards the sample edges and become narrower. It is an artifact of our TFA that, similar to the “perfect screening approximation” of Refs. [6] and [7], it yields ISs for any even-integer value of $\nu(x)$, possibly with extremely small width, provided the temperature is low and the collision broadening is small enough. If, for example, well developed ISs with local filling factor $\nu(x) = 4$ exist (in our case for $B \lesssim 3.6$ T), the TFA predicts the existence of additional narrow ISs with local filling $\nu(x) = 2$ close to the edges. The local equilibrium assumption requires that, in the limit $T \rightarrow 0$, $\gamma \rightarrow 0$, a part of the imposed current flows dissipationless through the ISs with $\nu(x) = 2$. While this has no effect on the vanishing of the longitudinal resistance R_ℓ in this limit, it leads for the Hall resistance to a value larger than $R_H = h/(4e^2)$, which is the value expected in the absence of the ISs with $\nu(x) = 2$. It is also an artifact of the TFA that, in the limit $T \rightarrow 0$, $\gamma \rightarrow 0$, the $\nu = 2$ QH plateau extends down to B -fields at which ISs with local $\nu(x) = 4$ occur (see black lines in Fig. 7, $\lambda = 0$). Of course, the accuracy of our calculation becomes insufficient, if the width of ISs becomes comparable with the separation of our mesh points.

To overcome these artifacts of the TFA, we introduce the averaged conductivity tensor, Eq. (8) [11]. Then the ISs become ineffective, if their width becomes less than 2λ . In Fig. 7 calculated values for Hall and longitudinal resistance are shown for several values of temperature, collision broadening, and imposed current, with λ taken as a multiple of the magnetic length ℓ_B . With increasing λ the ISs become ineffective at

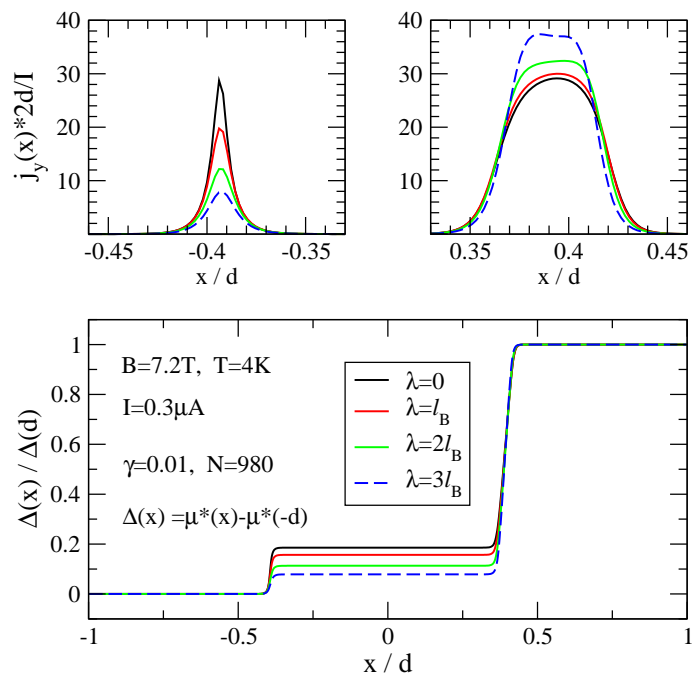


Figure 8. Effect of smoothing on current density and normalized Hall potential. $B = 7.2$ T.

higher B values, so the low- B edge of the QH plateaus occurs at larger B . Increasing temperature and collision broadening have a similar effect. However, small collision broadening leads to strongly reduced longitudinal resistance in the tails of Landau levels, see Eq. (6). This leads to large effects on both sides of the QH plateaus, whereas the other parameters have strong effects on the low- B side of the QH plateaus, but little effect on the high- B side. With increasing imposed current I the relevant IS becomes wider and, if the other parameters are fixed, the low- B edge of the plateaus shifts to lower B values.

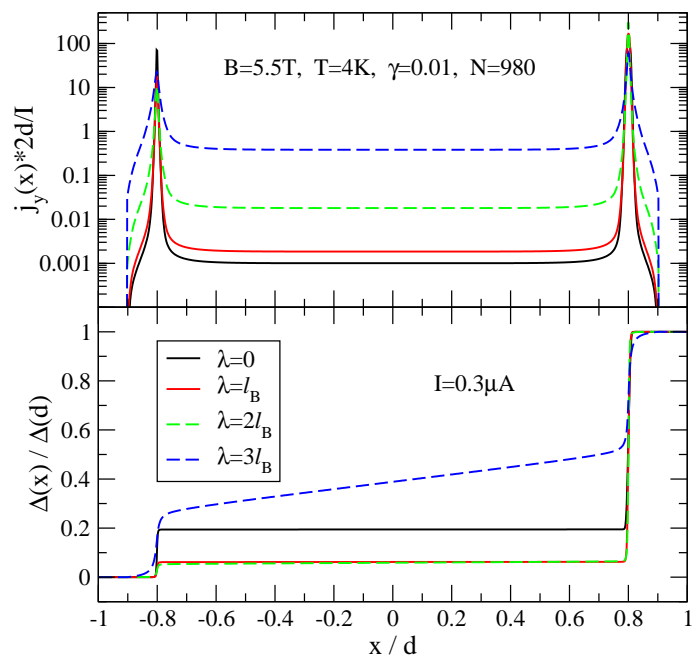


Figure 9. As Fig. 8, but for $B = 5.5$ T.

Depending on the width of the ISs, the smoothing of the conductivity can have different effects. For relatively broad ISs, as in Fig. 8 for $B = 7.2$ T, the smoothing just reduces the current through the narrow and increases the current through the broader strip, and thus increases the asymmetry. Figure 9 shows the corresponding results for $B = 5.5$ T, where the ISs are considerably narrower. For small λ the effect is similar to that in Fig. 8, but for larger λ the current density is reduced in both ISs and spreads out into the compressible region, resulting in a finite Hall field between the ISs and a breakdown of the QHE. An overview on the B -dependence of current distribution and variation of the Hall potential is given in Fig. 10. At high magnetic fields, $B \gtrsim 8$ T,

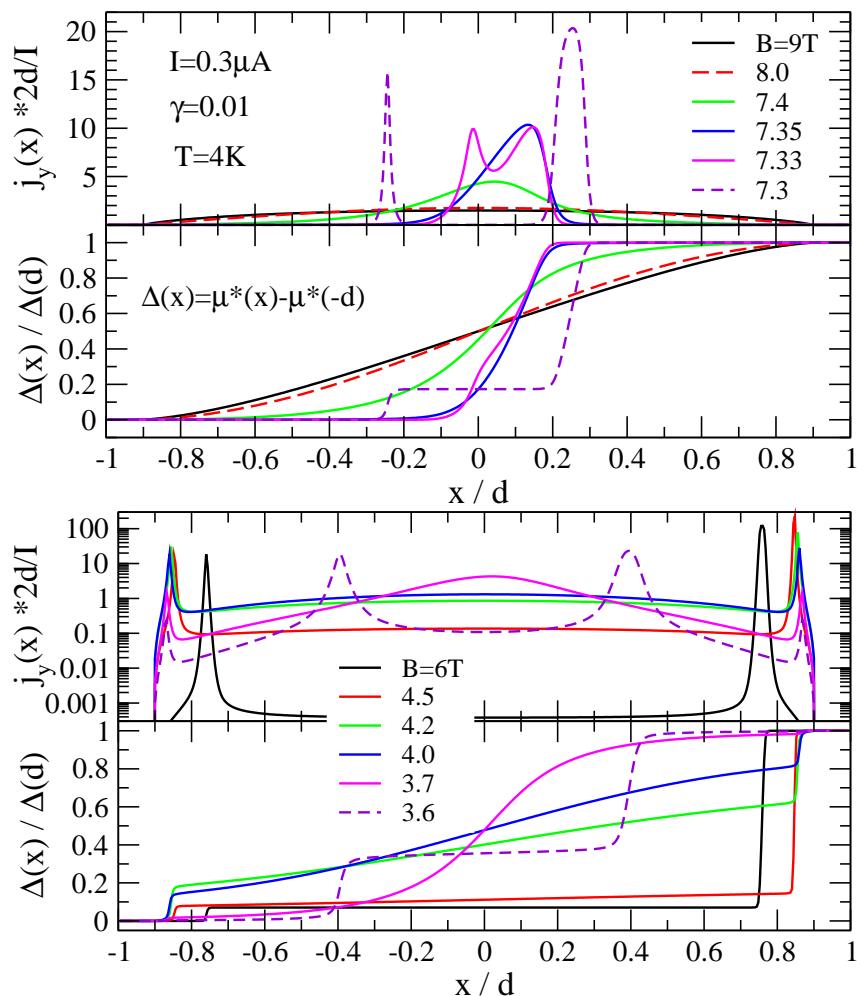


Figure 10. Distribution of imposed current and normalized Hall potential for several B values. $I = 0.3 \mu\text{A}$, $T = 4\text{K}$, $\gamma = 0.01$, $\lambda = \ell_B$.

only the lowest Landau level is partly occupied, there exist no ISs, and the current is spread out over the whole sample, so that the Hall potential varies nearly linearly, as in the Drude limit. As B is lowered and the filling factor in the center increases towards $\nu(0) \approx 2$, the current concentrates more and more in the center region, see the result for $B = 7.4$ T, until near $B = 7.35$ T an incompressible strip occurs in the center, and the current is essentially confined to that IS. With increasing current I , the peak of $j_y(x)$ becomes increasingly asymmetric, with the maximum on the side where I and the intrinsic current density have the same direction, as shown in Fig. 11. As B is

lowered further, the IS splits into two ISs, which rapidly separate spatially (see Fig. 10 for $B \leq 7.3$ T).

4. Discussion

The current-induced asymmetry, which has already been mentioned in Ref. [10], is due to the existence of incompressible strips, which develop at sufficiently low temperature and small collision broadening. At higher temperature and larger collision broadening the conductivity components are essentially proportional to the local density as in the Drude limit. Then the Hall electric field becomes constant, Eq. (3), and the Hall potential varies linearly over the sample. The self-consistent confinement potential gets a corresponding linear contribution, so that no major changes of the electron density result. At high magnetic fields, $B \gtrsim 8$ T, where only the lowest Landau level is partly occupied, the situation is similar, even at very low temperatures.

At low temperature and for small collision broadening, the local thermodynamic density of states is very large, where the electrochemical potential is close to a Landau level (LL), and very small otherwise, and the sample approaches the “perfect screening” situation [6, 7]. In a typical equilibrium situation, as shown in Figs. 2 and 3, with $\nu(0) \gtrsim 2$, in the center region the LL $n = 1$ is pinned to the constant μ^* , while in the outer regions near the edges, where $n_{\text{el}}(x)$ drops to zero, the lowest LL, $n = 0$, is pinned to μ^* . These “compressible” regions are separated by ISs, in which the eigenstates $|n, X\rangle$ carry the current $-e\langle n, X | \hat{v}_y | n, X \rangle = (e/m\omega_c)dE_n(X)/dX$. Since the potential energy varies across the ISs by $\hbar\omega_c$, in the right IS flows the dissipationless current $I_R = e\omega_c/\pi$ and in the left IS the opposite current $I_L = -I_R$. For $B = 7.2$ T, the

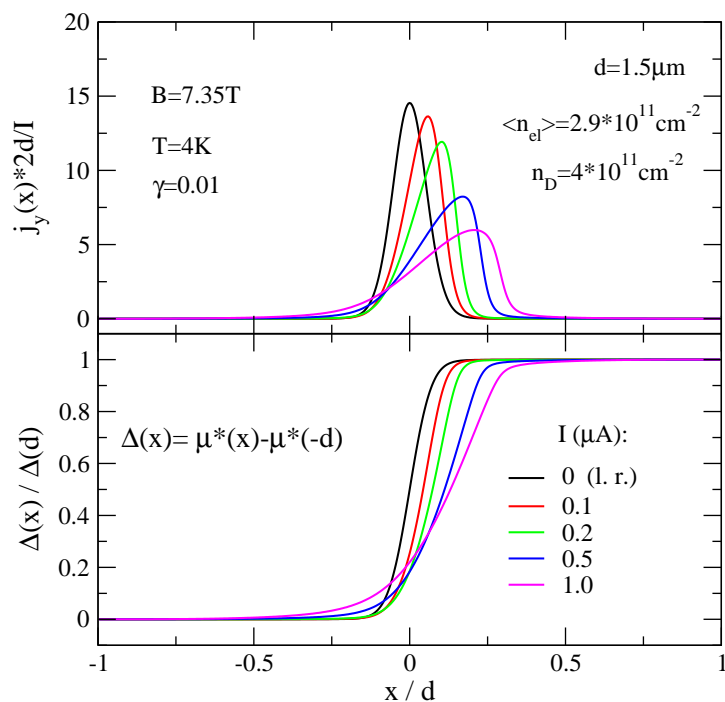


Figure 11. Distribution of imposed current and normalized Hall potential for $B = 7.35$ T and several I values. $T = 4$ K, $\gamma = 0.01$, $\lambda = \ell_B$.

Hall voltage across the right IS is $U_R = \hbar\omega_c/e = 12.46$ mV corresponding to a current $I_R = U_R/R_H(2) = 0.965$ μ A. If now an additional stationary current I^{ad} is imposed, the general rules of non-equilibrium thermodynamics require that the system assumes the stationary state with minimal entropy production, i.e. the additional current has to flow also dissipationless through the incompressible strips. For $I^{ad} > 0$ the current part $I_R^{ad} > 0$ will enhance the current through the right IS to $I_R + I_R^{ad}$ and the voltage drop across it to $U_R + R_H(2)I_R^{ad}$. The part $I_L^{ad} = I^{ad} - I_R^{ad} > 0$ reduces the intrinsic current through and the voltage drop across the left IS. Electrostatic arguments [6] show that the width w of an IS increases with the potential drop ΔV across it. Chklovskii *et al.* estimate $w^2 = a \cdot \Delta V$, where the constant a is inversely proportional to the slope of the (zero- B) density profile in the center of the IS [see Eq. (20) of Ref. [6]]. This predicts, that the IS, in which intrinsic and imposed currents have the same direction, becomes wider, whereas the width of the other IS, where the imposed current reduces the intrinsic one, is reduced. This prediction is confirmed by the self-consistent calculations. These show further, that the part I_L^{ad} of the imposed current flowing in the left IS, becomes equal to the other part I_R^{ad} in the linear response limit of small I^{ad} , whereas it becomes much smaller, $I_L^{ad} \ll I_R^{ad}$, for large I^{ad} . At higher temperature and for finite collision broadening, screening is not perfect and the “perfect screening” results hold only approximately. These non-linear transport effects are most important near the low- B edges of the QH plateaus.

Also the smoothing of the conductivity tensor is most effective near these edges. This smoothing has a strong effect on narrow ISs, where it removes the zeroes of $\sigma_\ell(x)$, but only a weak effect on wide ISs, where it mainly modifies the behavior near the edges. Thus it enhances the current-induced asymmetry, as is shown in Fig. 8. As discussed in Ref. [11] for the linear-response limit of weak imposed current, replacing of $\hat{\sigma}(x)$ by its average $\hat{\hat{\sigma}}(x)$ over an interval of length 2λ reduces the width of the QH plateaus, as shown in Fig. 7. Taking the averages with sufficiently large λ , makes the ISs with $\nu(x) = 2$ ineffective already at higher B -fields, for which no ISs with $\nu(x) = 4$ exist in the sample. Then the imposed current is spread out to the compressible region and suffers dissipation. Consequently, the QH plateau with $\nu = 2$ shrinks at its low- B side, where R_H decreases and R_ℓ becomes finite. This is shown in Fig. 7 for $\lambda = \ell_B$ and $\lambda = 2\ell_B$. We see that for finite imposed current the effects of λ , of the collision broadening described by γ , and of temperature are qualitatively similar as in the linear response regime $I \rightarrow 0$. In addition Fig. 7 shows that the current-induced asymmetry of the ISs, resulting in a broadening of one IS, tends to broaden the QH plateaus at their low- B edge and, consequently, to lower R_ℓ .

The high- B edge of the $\nu = 2$ QH plateau seems rather insensitive to changes of all these parameters except γ : if the collision broadening is reduced, R_ℓ becomes smaller. Nevertheless, as Fig. 11 shows, the imposed current induces an asymmetry and a broadening of the region, in which the Hall potential varies, even if the filling factor in the center is only slightly below 2, and the current is confined to the center region. This asymmetry disappears, however, rapidly as B increases above the high- B edge of

the plateau, as can be seen from the results for $B = 7.4$ T and $B = 3.7$ T in Fig. 10.

Our results are in reasonable agreement with the experiments [12, 13], where two cases could be distinguished. Near the low- B edges of the QH plateaus an “edge-dominated behavior” was found, in which most of the Hall potential dropped in an asymmetric way over relatively narrow stripes near the edges of the Hall bar. Near the high- B edges of the QH plateaus a “bulk-dominated behavior” was observed, with the major change of the Hall potential near the center of the Hall bar. The exact position of the potential drop changed along the bar, probably due to inhomogeneities. Such inhomogeneities make our assumption of translation invariance a crude approximation to reality, and may be the reason, why in the experiments the bulk-dominated situation is observed in a wider interval of B -values than in our results.

We find in the edge-dominated situations that the asymmetry of the Hall voltages across the ISs is connected with a difference in the widths of the ISs, notably with a remarkable broadening of the IS, which carries the larger current and leads to the larger step in the Hall potential. Whereas the asymmetry of the potential steps is clearly seen in the experiments, the current-dependence of the width of the corresponding strips is not clearly observed (see Fig. 1), possibly because of the restricted spatial resolution (~ 100 nm). The weak asymmetries seen in Fig. 11 do not contradict to the experimental results for weak imposed currents, but can also not clearly be confirmed by the experiments [12, 13]. At higher currents ($I \approx 3.9 \mu\text{A}$) the experimental curves change suddenly their shape [12], probably due to the breakdown of the QHE.

The breakdown of the QHE with increasing current can also be seen from Fig. 1, which shows that with increasing I the slope of the Hall potential in the compressible region between the ISs increases. Thus, a part of the current flows through the dissipative bulk, and the resistance is no longer quantized. Our results, on the other hand, say that with increasing I one of the ISs becomes wider, carries more current dissipationless, and leads to an extension of the QH plateau at its low- B edge. This points to a serious shortcoming of our approach: it does not consider breakdown effects, which may become relevant at high imposed currents. One of these effects is Joule heating, which will become important at these low temperatures, if the current flows, at least partly, through compressible, i.e. dissipative regions. Another one is the often discussed quasi-elastic inter-Landau-level-scattering (QUILLS) [18, 19], which must become important if, in strong in-plane electric fields, isoenergetic states of adjacent Landau bands tend to overlap spatially. Exactly this happens at the wide IS with the large potential step ΔV and the width $w \propto \sqrt{\Delta V}$. There the Landau energies have a slope $dE_n(X)/dX \approx \Delta V/w$, so that the spacing of the states $|0, X_0\rangle$ and $|1, X_1\rangle$ with equal energies $E_0(X_0) = E_1(X_1)$ is $|X_0 - X_1| = \hbar\omega_c w/\Delta V \propto 1/\sqrt{\Delta V}$, and becomes small as ΔV increases with increasing current I .

Apart from these well understood shortcomings of the existing calculations, the self-consistent screening theory provides a good understanding of the experimental results. The observed difference between “edge-dominated behavior” near the low- B edges of the QH plateaus and the “bulk-dominated behavior” near the high- B edges becomes

clear from Figs. 7 and 10. The edge-dominated behavior results from the two separated incompressible strips, which become narrower and less effective with decreasing B . But near the low- B edges of the QH plateaus, the ISs dominate the transport and, at fixed finite temperature, the longitudinal resistance decreases exponentially with increasing B throughout the whole plateau region (see Fig. 7). The bulk-dominated behavior, on the other hand, is determined by the B -value at which the population of a new Landau level starts. At slightly lower B -values an incompressible region exists in the center. At slightly larger B -values only the lower Landau level is nearly filled in the center of the sample, so that the resistivity there is very small. In both cases the center region determines the transport, which therefore is “bulk-dominated”.

A basic assumption of our explanation of the QHE in narrow Hall bars is, of course, that the lateral confinement of the 2DES introduces a position-dependence of the electron density, which decreases from a maximum in the center to zero near the edges of the sample.

Acknowledgments

We are grateful to Klaus von Klitzing for his continuing interest in and his support of this work.

References

- [1] Weitz P, Ahlswede E, Weis J, von Klitzing K and Eberl K 2000 *Appl. Surf. Sci.* **157** 349
- [2] Weitz P, Ahlswede E, Weis J, von Klitzing K and Eberl K 2000 *Physica E* **6** 247
- [3] Ahlswede E, Weitz P, Weis J, von Klitzing K and Eberl K 2001 *Physica B* **298** 562
- [4] Ahlswede E, Weis J, von Klitzing K and Eberl K 2001 *Physica E* **12** 165
- [5] von Klitzing K, Dorda G and Pepper M 1980 *Phys. Rev. Lett.* **45** 494
- [6] Chklovskii D B, Shklovskii B I and Glazman L I 1992 *Phys. Rev. B* **46** 4026
- [7] Chklovskii D B, Matveev K A and Shklovskii B I 1993 *Phys. Rev. B* **47** 12605
- [8] Lier K and Gerhardtts R R 1994 *Phys. Rev. B* **50** 7757
- [9] Oh J H and Gerhardtts R R 1997 *Phys. Rev. B* **56** 13519
- [10] Güven K and Gerhardtts R R 2003 *Phys. Rev. B* **67** 115327
- [11] Siddiki A and Gerhardtts R R 2004 *Phys. Rev. B* **70** 195335
- [12] Panos K 2011 *PhD thesis work* MPI Solid State Research, Stuttgart, *unpublished*
- [13] Panos K, Weis J, Gerhardtts R R and von Klitzing K *unpublished*
- [14] Siddiki A 2009 *Europhysics Letters* **87** 17008
- [15] Siddiki A, Horas J, Kupidura D, Wegscheider W and Ludwig S 2010 *New Journal of Physics* **12** 113011
- [16] Gerhardtts R R 2008 *phys. stat. sol. (b)* **245** 378
- [17] Gerhardtts R R 1975 *Z. Phys. B* **21** 285
- [18] Eaves L and Sheard F W 1986 *Semicond. Sci. Technol.* **1** 346
- [19] Güven K, Gerhardtts R R, Kaya I I, Sağol B E and Nachtwei G 2002 *Phys. Rev. B* **65** 155316